

## Planet Hunters VI: The First *Kepler* Seven Planet Candidate System and 13 Other Planet Candidates from the *Kepler* Archival Data<sup>1</sup>

Joseph R. Schmitt<sup>2</sup>, Ji Wang<sup>2</sup>, Debra A. Fischer<sup>2</sup>, Kian J. Jek<sup>7</sup>, John C. Moriarty<sup>2</sup>, Tabettha S. Boyajian<sup>2</sup>, Megan E. Schwamb<sup>3</sup>, Chris Lintott<sup>4,5</sup>, Arfon M. Smith<sup>5</sup>, Michael Parrish<sup>5</sup>, Kevin Schawinski<sup>6</sup>, Stuart Lynn<sup>5</sup>, Robert Simpson<sup>4</sup>, Mark Omohundro<sup>7</sup>, Troy Winarski<sup>7</sup>, Samuel J. Goodman<sup>7</sup>, Tony Jebson<sup>7</sup>, Daryll Lacourse<sup>7</sup>

joseph.schmitt@yale.edu

### ABSTRACT

We report the discovery of 14 new transiting planet candidates in the *Kepler* field from the Planet Hunters citizen science program. None of these candidates overlap with *Kepler* Objects of Interest (KOIs), and five of the candidates were missed by the *Kepler* Transit Planet Search (TPS) algorithm. The new candidates have periods ranging from 124 – 904 days, eight residing in their host star’s habitable zone (HZ) and two (now) in multiple planet systems. We report the discovery of one more addition to the six planet candidate system around KOI-351, marking the *first seven planet candidate system* from *Kepler*. Additionally, KOI-351 bears some resemblance to our own solar system, with the inner five planets ranging from Earth to mini-Neptune radii and the outer planets being gas giants; however, this system is very compact, with all seven planet candidates orbiting  $\lesssim 1$  AU from their host star. We perform a numerical integration of the orbits and show that the system remains stable for over 100 million years. A Hill stability test also confirms the feasibility for the dynamical stability of the KOI-351 system.

*Subject headings:* Planets and satellites: detection - surveys

---

<sup>1</sup>This publication has been made possible through the work of more than 250,000 volunteers in the Planet Hunters project, whose contributions are individually acknowledged at <http://www.planethunters.org/authors>. Individual participants who identified transits will be acknowledged in the final version of this paper.

<sup>2</sup>Department of Astronomy, Yale University, New Haven, CT 06511 USA

<sup>3</sup>Institute of Astronomy and Astrophysics, Academia Sinica Address: 11F of Astronomy-Mathematics Building, National Taiwan University. No.1, Sec. 4, Roosevelt Rd, Taipei 10617, Taiwan

<sup>4</sup>Oxford Astrophysics, Denys Wilkinson Building, Keble Road, Oxford OX1 3RH

<sup>5</sup>Adler Planetarium, 1300 S. Lake Shore Drive, Chicago, IL 60605, USA

<sup>6</sup>Institute for Astronomy, Department of Physics, ETH Zurich, Wolfgang-Pauli-Strasse 16, CH-8093 Zurich, Switzerland

<sup>7</sup>Planet Hunter

## 1. Introduction

Over the last 20 years, hundreds of exoplanets have been discovered. One powerful method to discover planet candidates is the photometric transit technique, in which a planet crosses in front of its host star as seen from Earth. The *Kepler* mission (Borucki et al. 2010) has been observing  $\sim 160,000$  stars nearly continuously for almost four years searching for these transit signals. In the first 12 quarters, spanning three years, more than 3,500 planet candidates have been discovered via this photometric transit technique<sup>1</sup> (Batalha et al. 2013, Burke et al. in prep.). The *Kepler* team searches for transit signals using a wavelet-based algorithm, the transit planet search (TPS) (Jenkins et al. 2002, 2010), which requires three transits with a significance of  $7.1\sigma$  to be placed on the Threshold Crossing Event (TCE) list, and has searched for periods up to 525 days (Tenenbaum et al. 2012). Those TCEs which pass additional tests, including a human review stage, become *Kepler* Objects of Interest (KOIs). It is expected that most of these KOI candidates are true planets (Morton & Johnson 2011). The false positive rate has been found to depend on the planet radius, with the lowest false positive rate ( $6.7 - 8.8\%$ ) in the range of  $1.25 - 6.00R_{\oplus}$ , where we find a majority of the new Planet Hunters candidates. Larger planets suffer a false positive rate of  $15.9 - 17.7\%$  (Fressin et al. 2013). However, the false positive rate for multiple planet candidates is very low, approximately only twos out of all *Kepler* targets (Lissauer et al. 2012).

While the TPS algorithm is clearly effective, some transit signals can be missed. The Planet Hunters (PH) project<sup>2</sup> (Fischer et al. 2012) is one of the Zooniverse projects<sup>3</sup> (Lintott et al. 2008, 2011; Fortson et al. 2012) and is designed to have humans visually check *Kepler* light curves, broken into 30 day increments, to search for transit signals missed by *Kepler*'s TPS algorithm. Since December, 2010, more than 250,000 public volunteers have searched through more than 19 million *Kepler* light curves hunting for transiting planets, contributing a cumulative total of 180 years of work.

While Planet Hunters has identified hundreds of transit signals, we only announce candidates that have not been listed as *Kepler* Object of Interest (KOI) candidates. Planet Hunters has discovered more than 40 new planet candidates (Fischer et al. 2012; Lintott et al. 2013; Wang et al. 2013; Schwamb et al. 2013), including two confirmed planets. The first confirmed planet from the PH project is PH1 b (Kepler-64b), a circumbinary planet in a  $\sim 137$  day orbit around an eclipsing binary, and is the first known planet in a quadruple star system (Schwamb et al. 2013). The second confirmed planet from the PH project is PH2 b (Kepler-86b), a gas giant planet residing in its host star's habitable zone (Wang et al. 2013). Statistical completeness analysis within the Planet Hunters project is performed by injecting fake transit events into real *Kepler* light curves (Schwamb et al. 2012). This analysis shows that Planet Hunters are effective at detecting transits

---

<sup>1</sup><http://exoplanetarchive.ipac.caltech.edu>, last accessed September 23, 2013

<sup>2</sup><http://www.planethunters.org/>

<sup>3</sup><https://www.zooniverse.org/>

of Neptune-sized planets or larger ( $\gtrsim 85\%$  completeness for short periods,  $P < 15$  days), although smaller planets can still be recovered.

In this paper, we present 14 total new candidates from Planet Hunters project. These discoveries include two candidates which are (now) in multi-planet systems and eight in the habitable zone. The additional planet candidate we detect in the known KOI six candidate system, KOI-351, marks the discovery of the *first Kepler* star with a seven planet candidate system. Section 2 explains how these new planet candidates were discovered. Section 3 explains our method to calculate the transit parameters, stellar parameters, and equilibrium temperature as well as a discussion of the false positives tests that we have carried out for our new planet candidates. Section 4 discusses characteristics of notable new candidates, such as whether the new candidate is in a multi-planet system or missed by the TPS algorithm. We conclude in Section 5.

## 2. Planet Hunters Candidate Discoveries

Candidates are identified through one of two ways. The classic method is through Planet Hunters interface (see, e.g., Fischer et al. 2012; Schwamb et al. 2012; Lintott et al. 2013), in which users are shown a 30-day light curve and asked to identify transit-like features. We have implemented a weighting scheme (Schwamb et al. 2012) in order to rank the quality of user transit classifications. In brief, all users start out with an equal weight, and synthetic light curves are used to seed the user weighting. Users who properly identify synthetic transits are given higher weights. The user weightings continue to evolve depending on whether or not individual rankings agree with the majority rankings. Transits above a threshold score are then sent to the science team to be analyzed.

The other way candidates are identified is via the Planet Hunters Talk page<sup>4</sup>. This discussion tool allows users to publicly post and discuss interesting light curves with others. It is through this interface that users are easily able to download all data and collectively scrutinize potentially interesting light curves. The interface provides quick links to the MAST<sup>5</sup>, SkyView<sup>6</sup>, and UKIRT databases for each object. Tutorials for light curve analysis through the publicly available web-based tools hosted at the NASA Exoplanet Archive (NEA) are used frequently to calculate periodograms, normalize, and phase-fold the data, as well as performing data validation to rule out false positives. PH volunteers are *instrumental* in the success of the Planet Hunters project. Collections of possible planet candidates made by volunteers are passed to the Planet Hunters science team routinely for further analysis, follow-up, and scientific publication. This paper reflects discoveries made through the Planet Hunters Talk interface.

---

<sup>4</sup><http://talk.planethunters.org>

<sup>5</sup><http://archive.stsci.edu/kepler/>

<sup>6</sup><http://skyview.gsfc.nasa.gov/>

As described previously, the automated transit detection TPS algorithm was run on *Kepler* data taken over quarters 1 – 12, identifying over 18,000 possible planetary candidates in the data known as threshold crossing events (TCE’s). We present five candidates missed entirely by the TPS algorithm: KIC 2437209, 5094412, 6372194, 6805414, and KIC 11442793 (KOI-351.07). The other candidates reported here do not meet the minimum threshold requirements (three or more transits) for a transit detection during the time baseline of quarters 1 – 12 when the TPS was last employed. They are: KIC 5010054, 5522786, 5732155, 6436029, 9662267, 9704149, 10255705, 11152511, 12454613.

### 3. Transit Characterization

#### 3.1. Data Validation

Once a system is identified as having a possible transit signal, we perform a full analysis of the system using the *Kepler* light curve (data validation; Batalha et al. 2010) and any other publicly available archival data. This includes using the PyKE package (Still & Barclay 2012) and screening the surrounding field for background eclipsing binaries (BGEB) through the target pixel files as well as ensuring that the flux-weighted centroid remains stationary during an object’s transit (Bryson et al. 2013). We use UKIRT and 2MASS images to search for nearby contaminating sources and asymmetric point spread functions, necessary for probing nearby unresolved sources due to the low-resolution of the *Kepler* CCD detector. The light curves are then fully modeled and inspected for variations in even-odd transit depth, the presence of secondary eclipses, and misshaped transit profiles, any of which can indicate a falsely identified planetary candidate.

#### 3.2. Stellar Properties

The *Kepler Input Catalog* (KIC) provides estimates of the stellar parameters ( $T_{\text{eff}}$ ,  $\log(g)$ ,  $[\text{Fe}/\text{H}]$ ,  $R^*$ , spectral type) of all the stars in the Kepler field (Brown et al. 2011). However, these parameters not only have large intrinsic errors, but have been shown to have significant systematic errors as well (Basu et al. 2012; Verner et al. 2011; Muirhead et al. 2012; Pinsonneault et al. 2012). Fortunately, the design of the database for the *Kepler* stellar data hosted at the NEA is flexible to the introduction of modified stellar parameters as more precise observations and methodology become available. Table 1 lists the primary stellar parameters as well as the provenance<sup>7</sup> for each of our candidates.

We use the values in Table 1 as inputs for our own transit fitting routine (Wang et al. 2013) de-

---

<sup>7</sup>The “Provenance of Stellar Parameters” is described in the documentation available from the NEA website: [http://exoplanetarchive.ipac.caltech.edu/docs/API\\_keplerstellar.html](http://exoplanetarchive.ipac.caltech.edu/docs/API_keplerstellar.html).

veloped to iterate between the light curve solution and the Yonsei-Yale (Y<sup>2</sup>) Isochrones (Demarque et al. 2004) for a range of ages spanning from 0.08 – 15 Gyr, with  $[\alpha/\text{Fe}] = 0$ . We ran 1000 trials of Monte Carlo simulations using the Y<sup>2</sup> Isochrones to obtain stellar properties such as mass, radius and luminosity. The distributions of the inputs are assumed to follow a Gaussian function. The mean and standard deviation are the reported value and error bar in the KOI table. The distributions of the outputs are used to constrain the transit light curve fitting, excluding mathematically acceptable fittings that are physically unlikely. The formal error bars sometimes result in unrealistically low error bars for  $\log(g)$ , so we adopt a floor on the  $\log(g)$  error bar of  $\pm 0.10$ . The outputs of the transiting light curve fitting (e.g., stellar density) can also be used to constrain the Y<sup>2</sup> Isochrone. Thus, the iterative transit fitting routine is able to provide a set of self-consistent stellar and orbital solutions.

### 3.3. Transit Fitting

All available long-cadence light curves from *Kepler* quarters 0-16 were flattened, normalized, and phase-folded. We used a custom-made package (Wang et al. 2013) to find the best fit values for the orbital period ( $P$ ), the ratio of the planet radius to the stellar radius ( $R_{PL}/R_*$ ), the ratio of the semi-major axis to the stellar radius ( $a/R_*$ ), inclination ( $i$ ), eccentricity ( $e$ ), longitude of periastron ( $\omega$ ), and midtransit times. Quadratic limb darkening parameters are determined by interpolating a table provided by Claret & Bloemen (2011). The best fit parameters were determined through a Levenberg-Marquardt least square algorithm, while the error bars are estimated with a bootstrapping method by which data points are perturbed according to the photometric uncertainty and initial guesses are perturbed according to the standard deviation of the previous runs.

The phase-folded solutions for each star are shown in Figure 1. Odd and even transits are colored blue and red, respectively, and there is no significant odd-even depth variation, which would be indicative of an eclipsing binary star system. Table 2 contains best fit parameters for the new planet candidates.

### 3.4. Equilibrium Temperature

Each planet’s equilibrium temperature ( $T_{\text{PL}}$ ) is calculated based on the best fit  $a/R_*$  from the transit model and the stellar effective temperature as determined in Section 3.2 according to the following equation:

$$T_{\text{PL}} = T_{\text{eff}} \cdot \left(\frac{1 - A}{4}\right)^{\frac{1}{4}} \cdot \left(\frac{a}{R_*}\right)^{-\frac{1}{2}} \quad (1)$$

where  $A$  is Bond albedo (Seager 2010). We arbitrarily set  $A = 0.30$ , which is approximately equal

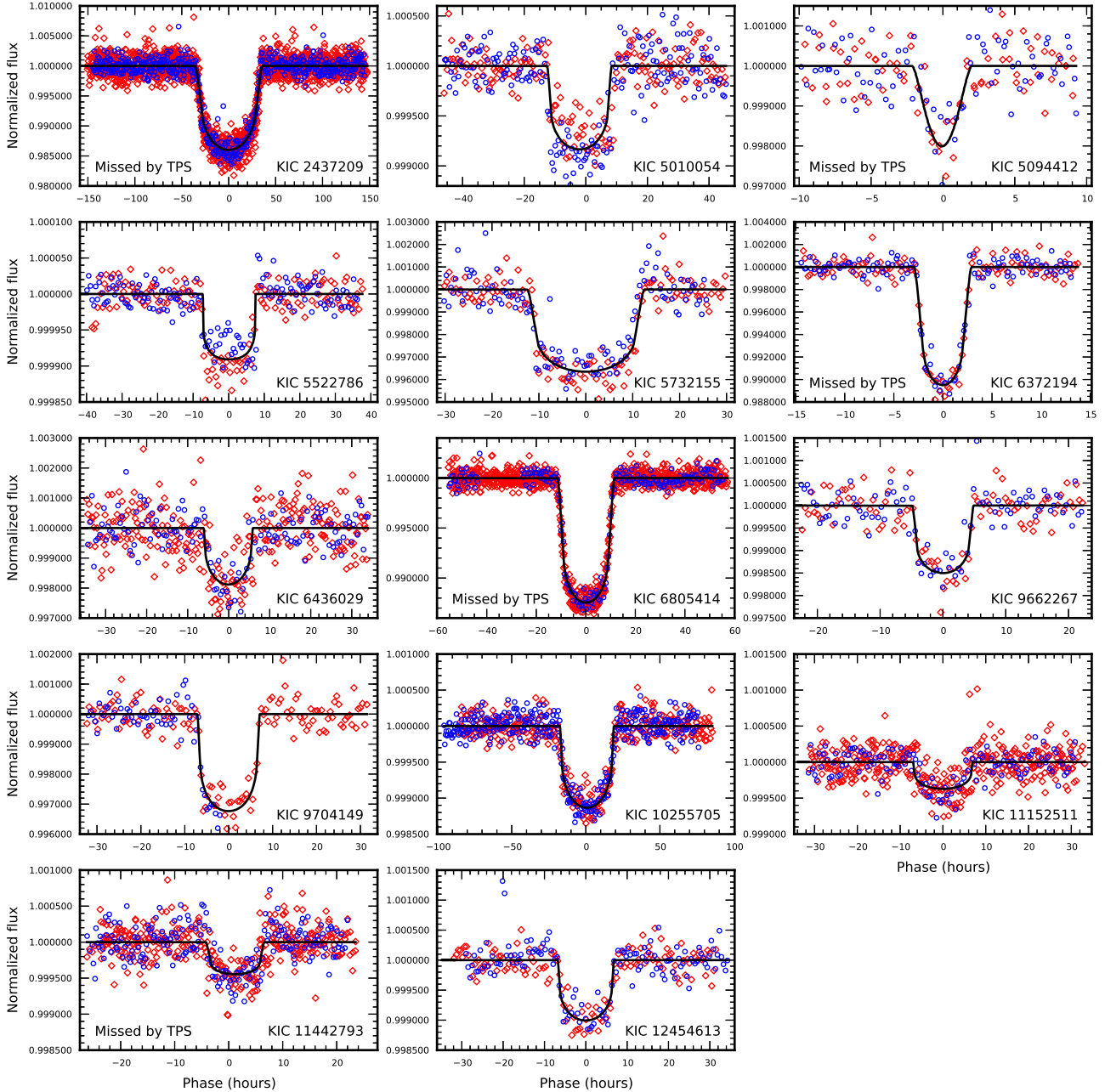


Fig. 1.— Phase-folded transit models for new Planet Hunters candidates. Blue squares represent odd transits and are overplotted onto the red squares, which represent even transits. There are no significant differences between the depths of the even and odd transits for any candidate. Candidates missed by the TPS algorithm are KIC 2437209, 5094412, 6372194, 6805414, and KIC 11442793 (KOI-351.07). See Section 3.3 for details.

to the values for Uranus ( $A = 0.300$ ) and Neptune ( $A = 0.290$ ). In this calculation, we assume zero eccentricity, as transit fitting for eccentricity is generally poorly constrained and has large error bars usually consistent with 0. This approximation should not significantly affect the candidates with moderate eccentricities, but may significantly affect the more highly eccentric candidates. Defining the edges of the HZ to be 185 K and 303 K per Batalha et al. (2013), eight of our planets are in the HZ, and two others are within  $1\sigma$  of the HZ (Figure 2).

#### 4. New Planet Candidates

The best-fit parameters for the 14 new planet candidates in this paper are listed in Table 2. Their periods and radii are plotted in Figure 3. Comments on individual candidates are given below.

##### 4.1. KIC 2437209

In quarters 1 – 16, the light curve for KIC 2437209 has four large ( $\sim 14000$  ppm) and long transits (duration of 71 hours; see Figure 1, Table 2). Although this star had three transits in quarters 1 – 12, it was missed by the TPS pipeline. This is likely due to moderate light curve variability during the first transit, which, combined with the long duration, hampered TPS’s ability to detect the transit.

KIC 2437209’s 71 hour transit duration, approximately equivalent to the duration of Neptune transiting the Sun, is extremely long for a 281 day period planet. Our first attempts at modeling this system resulted in a degeneracy in the stellar and planetary radius. This system was consistent with two scenarios: a star on the giant branch with a stellar companion in a circular orbit or with a main sequence dwarf with a planetary companion in a highly eccentric  $e = 0.98$  orbit viewed at apastron, an unfavorable probability of occurrence. In the giant star interpretation, the stellar parameters were  $\log(g) = 2.95^{+0.13}_{-0.10}$ ,  $R^* = 5.30^{+0.98}_{-0.97}R_{\odot}$ ,  $T_{\text{eff}} = 4675^{+116}_{-197}K$ ,  $R_{PL} = 61.86 \pm 11.46R_{\oplus}$ ,  $e = 0$ , while the dwarf interpretation had values similar to the KIC values of  $\log(g) = 4.498$ ,  $R = 0.844R_{\odot}^*$ ,  $T_{\text{eff}} = 4655K$ ,  $[\text{Fe}/\text{H}] = -0.047$ ,  $R_{PL} = 13.26 \pm 10.22R_{\oplus}$ ,  $e = 0.98$ .

This degeneracy led us to obtain one spectrum of the star with Keck/HIRES (Vogt et al. 1994) in an attempt to better determine the stellar parameters. We used Spectroscopy Made Easy (SME) (Valenti & Piskunov 1996; Valenti & Fischer 2005) to model the spectrum; however, due to the faintness of the star ( $K_p = 16.353$ ) the resulting signal to noise ratio (SNR) was  $\sim 15$ , well below the preferred regime for reliable SME analysis. Nevertheless, our results fitting the spectrum with SME gave  $T_{\text{eff}} = 4965 \pm 100K$ ,  $\log(g) = 3.75 \pm 0.2$ , and  $[\text{Fe}/\text{H}] = 0.564 \pm 0.10$ , which is inconsistent with both the  $Y^2$  model and the KIC values.

KIC 2437209 has six quarters of short-cadence data and likely belongs to the open cluster

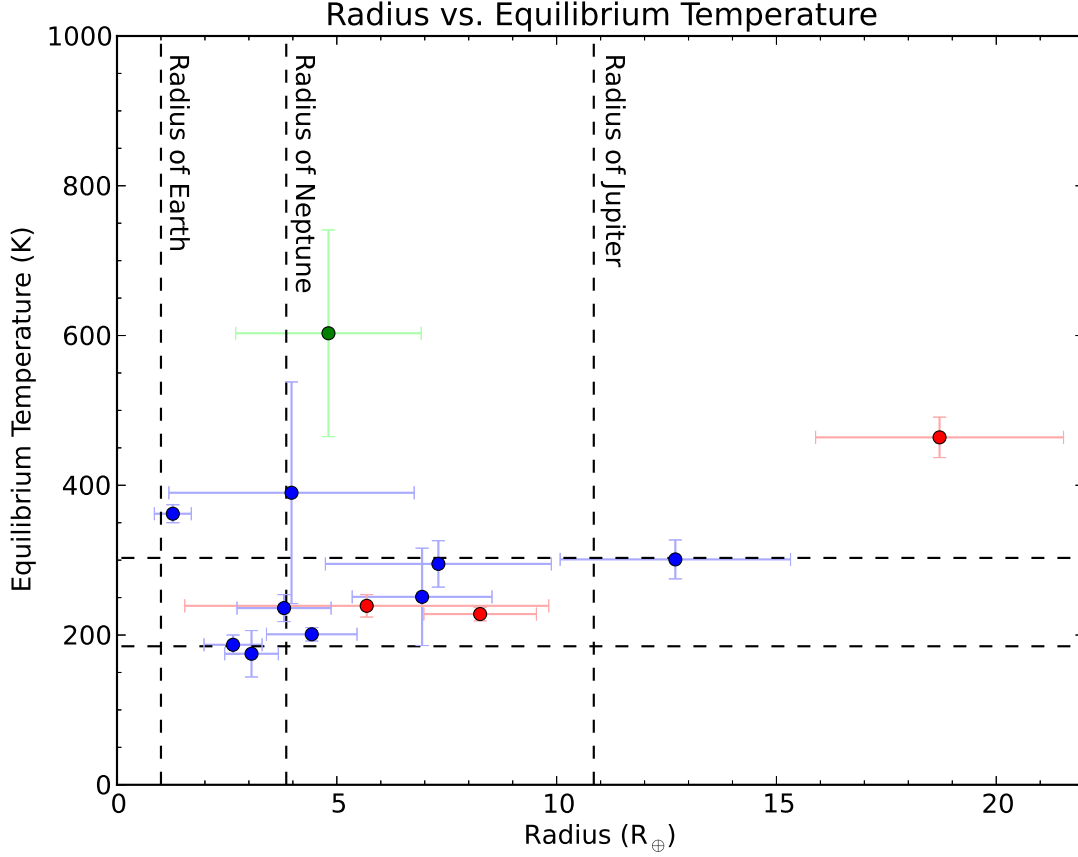


Fig. 2.— The equilibrium temperature vs. planet radius for the new Planet Hunters candidates. Red points are the new candidates that TPS missed, and the green point is KOI-351.07, which was also missed by TPS. Blue candidates are those which TPS should not have detected: those candidates with fewer than three transits in quarters 1 – 12. Eight new planets are in the HZ (185 – 303K), and two others are within  $1\sigma$  of the HZ. For convenience, the candidate around KIC 2437209 is not shown ( $P = 281.22$  days,  $R = 61.86 \pm 11.46R_{\oplus}$ , duration= 71.24 hours; see Section 4.1 for details), which was also missed by TPS.



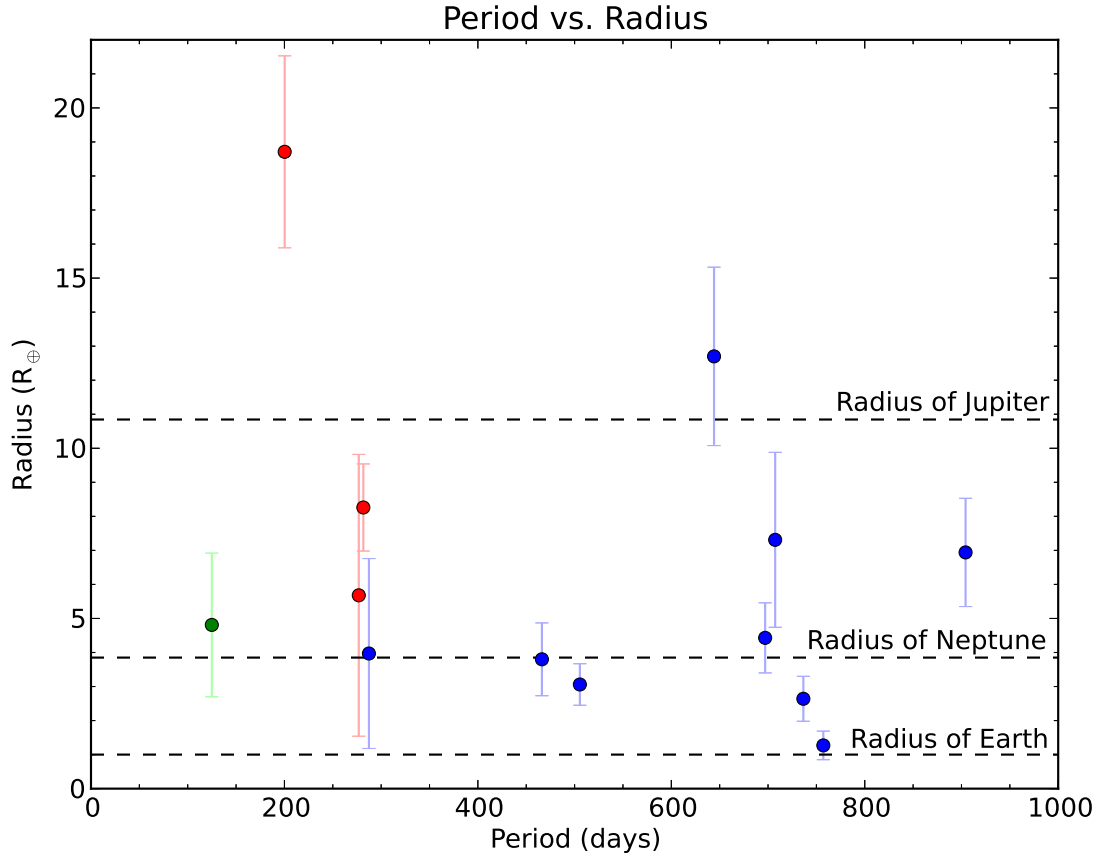


Fig. 3.— The radius vs. period for the new Planet Hunters candidates presented in this paper. Red points are the new candidates that TPS missed, and the green point is KOI-351.07, which was also missed by TPS. Blue candidates are those which TPS should not have detected: those candidates with fewer than three transits in quarters 1 – 12. For convenience, the candidate around KIC 2437209 is not shown ( $P = 281.22$  days,  $R = 61.86 \pm 11.46R_{\oplus}$ , duration= 71.24 hours; see Section 4.1 for details), which was also missed by TPS.

NGC 6791. Evolved cluster stars are usually targets for short-cadence *Kepler* observations to study pulsations. However, given its faint magnitude, we believe that this target was added to the short cadence list by mistake because it is far too faint for asteroseismology (Daniel Huber, private communication). With  $g' = 17.239$  and  $(g' - r') = 1.001$  given by the *Kepler Input Catalog*, KIC 2437209 is placed on the giant branch of NGC 6791 on the  $g'$  vs.  $(g' - r')$  color-magnitude diagram (Platais et al. 2011). Therefore, KIC 2437209 is very likely to be a giant star with a smaller stellar companion. However, should this planet indeed have  $e = 0.98$ , then this planet may be one of the super-eccentric planets predicted in Socrates et al. (2012) caught in the act of high eccentricity migration.

#### 4.2. KIC 5094412

KIC 5094412 has the shortest transit duration of our candidates (3.20 hours), leading to few in-transit data points. We note that two of the four transits appear V-shaped (without an even-odd difference), a shape that can be produced by a grazing EB system. However, the actual transit morphology of this system is unclear due to the under-sampling induced by the short duration transits. This is the only candidate in our sample that has such a potential V-shaped transit profile. KIC 5094412 has three transits within quarters 1 – 12, but was missed by the TPS pipeline.

#### 4.3. KIC 5522786

KIC 5522786 has only two transits and both exhibit a very sharp ingress and egress. This is the second smallest candidate in this paper, a near super-Earth sized planet of  $R = 1.27 \pm 0.42 R_{\oplus}$ . Despite a depth of only  $91 \pm 13$  ppm, the transits are visually apparent due to the host star’s brightness, a Kepler-magnitude = 9.350 star. A third transit of this candidate would be extremely valuable and is expected to take place at about 2456630.6144 JD (December 4, 2013). We also note that the star has the highest effective temperature in our sample with  $T_{\text{eff}} = 8725^{+191}_{-184} K$ .

#### 4.4. KIC 6372194

KIC 6372194 is fairly faint, with a Kepler magnitude of 15.870. The light curve for KIC 6372194 lacks any sign of stellar variability, and transit depths are very large with an approximate 1% dip in light. This candidate has three transits within quarters 1 – 12, but was missed by the TPS pipeline.

#### 4.5. KIC 6436029

KIC 6436029 already has one KOI candidate (KOI 2828.01;  $P = 59.5d$ ,  $R = 4.1R_{\oplus}$ ). We have detected three transits of another planet around this star with  $P = 505.45d$ . This new planet lies in the HZ and has  $R = 3.06 \pm 0.61R_{\oplus}$ .

#### 4.6. KIC 6805414

KIC 6805414 has a 1.2% dip in brightness with a period of 200.25 days. The best fit shows a radius  $18.71 \pm 2.82R_{\oplus}$ , which is on the upper edge of the planetary regime. Curiously, despite having four obvious transit signals before Q12 and another partial transit at the end of Q9 which are easily distinguishable from the moderate light curve variability, this signal is not reported as either a TCE or a KOI.

#### 4.7. KIC 11442793

KIC 11442793 has six listed KOI candidates (KOI-351) at periods of 7.01, 8.72, 59.74, 91.94, 210.61, and 331.64 days (see Table 4 for transit parameters). Planet Hunters has detected an additional 124.92 day signal with five full transits and one partial transit. However, after the first transit (Quarter 2), the next transit fell within a data gap. The following transit contained only the egress due to a data gap within Q5. The two subsequent transits also fell into data gaps. However, despite four consecutive transits likely being missed by TPS, there were still three full transits (and the partial) occurring during the first 12 quarters of *Kepler*, meaning this should have been detected. TPS may have run into problems due to too many transit signatures. According to Tenenbaum et al. (2010), after four candidates are found, the TPS algorithm skips to the next target star. There are currently (as of September 23, 2013) four TCEs listed for KIC 11442793. Two of them are aliases of KOI-351.03 ( $P = 59.74$  days) at  $P = 179.214$  and  $P = 238.944$  days. It is possible that these aliases prevented TPS from finding the 124.92 day signal.

To test whether the seventh signal is merely an alias of one or more of the previous six candidates, we assumed a linear ephemeris for all planets and calculated each planet’s midtransit points (see Table 3). None of the planets matched the seventh candidate. In fact, somewhat surprisingly, *only one* midtransit of the previously known six planet candidates comes within 24 hours of a midtransit of the seventh candidate, but unsurprisingly, it’s the candidate with the shortest period (7.01 days). However, we recognize the fact that we cannot assume a perfectly linear ephemeris on account of transit timing variations, or TTVs (Miralda-Escudé 2002; Agol et al. 2005; Holman & Murray 2005; Holman et al. 2010).

Indeed, we quickly analyzed the system using the IDL program TAP (Carter & Winn 2009; Gazak et al. 2011; Eastman et al. 2013) to determine transit midpoints and compared the observed

midtransits to the midtransits expected from the KOI epochs and periods. A plot of the observed midtransit times minus calculated midtransit times ( $O - C$ ) shows deviations from a perfectly linear ephemeris due to TTVs for the outer three planets, indicating significant gravitational interactions between planets. Figure 4 shows the  $O - C$  plot for the outer three planet candidates of KOI-351. The last transit of KOI-351.02 has  $O - C = +14.4$  hours, while the second-to-last transit has  $O - C = -9.4$  hours, a change of 24 hours over the course of one period. KOI-351.02 has one of the largest TTVs known, excluding circumbinary planets (Mazeh et al. 2013). The presence of TTVs significantly increases the likelihood that our planet candidates are real, as they show mutual gravitational interactions with their neighbors. A more in-depth analysis can likely be used to determine masses and confirm several planets in this system, but this is left for future studies.

Because we cannot rely solely on comparisons of linear ephemerides, we also compared the transit depths and transit durations of all seven candidates. The transit depth for KOI-351.07,  $446 \pm 93$  ppm, is only consistent with two of the KOI candidates, KOI-351.03 and KOI-351.04, but the duration of the 7th candidate is hours longer than either. These two candidates also have *significantly* different midtransit times and thus cannot be the same object as KOI-351.07. The depths and durations are compared in Table 3, which also shows the phase information of each KOI-351.07 transit relative to the other six candidates. If KOI-351.07 were in fact a secondary eclipse from one of the other six objects, we would see a constant phase offset of KOI-351’s transit relative to the primary eclipses. No such phase offset is observed. A combination of looking at the differences in duration, depth, midtransit points, and phases of KOI-351.07 relative to the other six candidates clearly demonstrates that KOI-351.07 is a distinct object. Simply put, the seventh candidate is not an alias of any of the other six candidates.

We also performed two stability tests to assess the feasibility of this system. Hill stability is a simple stability diagnostic that can be used to determine whether this somewhat compact system is at least feasible. Following the method of Lissauer et al. (2011b), we calculate masses according to  $M = R^{2.06}$  (in Earth units) and their mutual Hill sphere radii. If

$$\Delta = \frac{a_{\text{outer}} - a_{\text{inner}}}{R_H} > 2\sqrt{3} \approx 3.46 \quad (2)$$

then the planets are Hill stable, which means that the two planets will never cross orbits, assuming zero eccentricity. However, this determination is highly dependent on stellar radius due to the assumed planet mass-radius relationship; it is also somewhat dependent on stellar mass. The best fit values for these two parameters from  $Y^2$  interpolation are  $R = 1.14_{-0.13}^{+0.07} R_\odot$  and  $M = 1.13_{-0.18}^{+0.09} M_\odot$ , which are consistent with the KOI values of  $R = 1.07 \pm 0.46 R_\odot$  and  $M = 1.14 \pm 0.12 M_\odot$ .

Because of the extremely large TTVs, we might expect that the mutual Hill spheres of the outer two planets are very close to the Hill stability criterion (see Equation 2). As expected from the TTVs, the least Hill stable pair of planets are KOI-351.01 ( $P = 331.6$  days) and KOI-351.02 ( $P = 210.6$  days), the outer two planets. All other planet pairs remain Hill stable across the  $2\sigma$  range of stellar radius and mass. At the best fit  $Y^2$  value for stellar mass and radius,  $\Delta = 3.78$  for

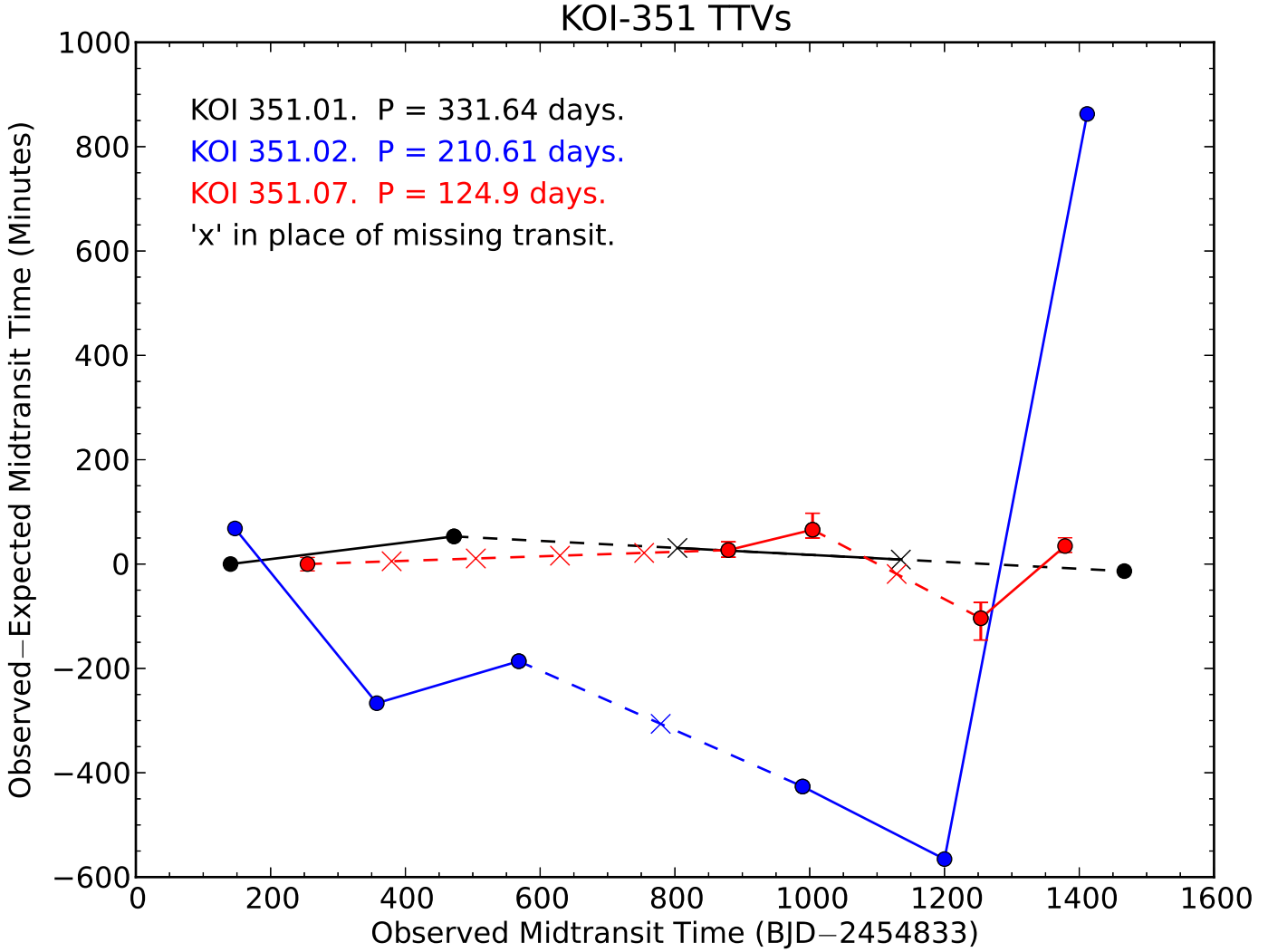


Fig. 4.— Observed–Calculated ( $O - C$ ) midtransit times for the outer three planet candidates of KOI-351: KOI-351.01 in black, KOI-351.02 in blue, and KOI-351.07 in red. An ‘x’ corresponds to the approximate time a transit was expected to occur, but was missed due to a data gap. Solid lines are used to connect consecutive observed transits, while dashed lines are used to connect non-consecutive observed transits. Error bars are plotted and are smaller than the markers where not seen. The  $O - C$  of the last midtransit of KOI-351.02 is 24 hours larger than the  $O - C$  of the second-to-last midtransit of KOI-351.02, making KOI-351.02’s TTVs one of the largest known (Mazeh et al. 2013). The presence of TTVs increases the likelihood that the planets are real and within the same system.

outer pair, just above the stability criterion. Holding  $M^*$  constant and increasing  $R^*$  (increasing planet radius and therefore mass), the system remains Hill stable ( $\Delta \geq 3.46$ ) until  $R \approx 1.31R_\odot$ , just above the  $2\sigma$  error in  $R^*$ . Holding  $R^*$  constant and decreasing  $M^*$  (increasing  $M_{PL}/M^*$  ratios and lowering the semimajor axis separations), the system remains Hill stable until  $M \approx 0.87M_\odot$ , which is  $1.4\sigma$  below the best fit. This leaves open a wide parameter space for a Hill stable system to exist.

Lastly, we ran an orbital integration using the best fit values; the system was stable for  $> 100$  Myr. However, this was only a feasibility test and is by no means an exhaustive analysis proving dynamic stability, yet the fact that the outer three planets all exhibit TTVs is a major indicator that all three planet candidates orbit the same star.

Lissauer et al. (2012) finds that “almost all of *Kepler*’s multiple planet candidates are planets” and shows that the expected number of *Kepler* stars with an astrophysical false positive decreases with the number of planet candidates in a system, decreasing below one for *Kepler* systems of 3+ planets. We have demonstrated that there are seven unique signals for KOI-351, that stability is feasible, and that TTVs exist for the outer 3 planets. Therefore, we state with the strongest level of confidence short of official confirmation that this is a true seven planet system.

KOI-351 is also interesting as it is close to being a compact analog to the solar system. The nominal radius values of the inner five planet candidates are all in the Earth to mini-Neptune regime ( $\lesssim 3.0R_\odot$ ), while the outer two candidates are gas giants. This differs from Kepler-11 (Lissauer et al. 2011a), in that all of Kepler-11’s planets are in the super-Earth to Neptune sizes. However, we stress that the error bars on the KOI-351’s stellar radius and thus the planetary radii are very large at roughly 50% each. The new candidate has a radius of  $R = 2.80 \pm 1.10R_\oplus$ . KOI 351 deserves a strong follow-up observation to better constrain the radii, analyze the TTVs, and confirm these planets. This new candidate also exemplifies how complicated signals that may confuse or overload computers can be deciphered by visual checks. We also note that Planet Hunters had independently discovered the 8.72 and the 91.94 day signals. However, in preparation of this paper, both were upgraded to KOI candidate status.

#### 4.8. Candidate Summary

To summarize, we discovered a seventh planet candidate around KOI 351, the first known *Kepler* system with seven candidates. We also added one new planet candidate to a known single planet system. There were five new planet candidates which should have been detected by the TPS algorithm, but were missed.

## 5. Conclusions

Planet Hunters is designed as a complementary check to the *Kepler* team’s own planet search algorithm, TPS. The TPS algorithm has been extremely successful with over 18,000 TCEs and over 3,000 candidates discovered. However, as shown by Planet Hunters, it is not 100% complete, even in cases that can be easily detected. TPS may find a signal, but misidentify the period due to not properly detecting all the transits, or it may miss detections altogether. As Planet Hunters only approaches completeness above roughly Neptune-sized planets (Schwamb et al. 2012), we cannot fully recover signals missed by TPS. As such, the completely new candidates missed by TPS are generally much larger than  $1R_{\oplus}$ : they have periods and radii of ( $P = 281.22$ ,  $R = 61.86 \pm 11.46R_{\oplus}$ ), ( $P = 276.88d$ ,  $R = 5.68 \pm 4.14R_{\oplus}$ ), ( $P = 281.58d$ ,  $R = 8.26 \pm 1.28R_{\oplus}$ ), ( $P = 200.25d$ ,  $R = 18.71 \pm 2.82R_{\oplus}$ ), and ( $P = 124.92d$ ,  $R = 2.80 \pm 1.10R_{\oplus}$ ).

The most important discovery presented here is the addition of one new planetary candidate around KOI-351, a known six planet candidate system. According to <http://exoplanets.org/> (Wright et al. 2011), the two stars with the largest number of confirmed planets, excluding our Sun, contain six planets each: HD 10180 (Lovis et al. 2011) and Kepler-11 (Lissauer et al. 2011a). Furthermore, there are currently only five exoplanetary systems with five confirmed planets: 55 Cancri (Fischer et al. 2008), Kepler-20 (Borucki et al. 2011; Fressin et al. 2012), Kepler-32 (Borucki et al. 2011; Swift et al. 2013), Kepler-33 (Borucki et al. 2011; Lissauer et al. 2012), and Kepler-62 (Borucki et al. 2013). There are also 14 stars with 5+ KOI planet candidates that have not yet been validated (as of September 23, 2013). Although HD 10180 has been claimed to have seven (Lovis et al. 2011) to nine (Tuomi 2012) potential planetary signals, and GJ 887C is claimed to have up to seven potential planetary signals (Anglada-Escudé et al. 2013), their existence remains highly uncertain. Conversely, we believe that KOI-351 is a true seven planet system with the highest level of certainty short of official confirmation. Analysis shows that this seventh signal is not an alias of the other six and is feasibly stable. Large TTVs for the outer two planet pairs strongly indicate that the outer two planet pairs are likely interacting gravitationally, which helps to validate the system. It is also well known that candidates in multiple candidate systems have much lower false positive probabilities than single candidate systems (Lissauer et al. 2012).

KOI-351’s system looks somewhat like our own, but much more compact; all seven planet candidates are  $\lesssim 1$  AU from their host star. While the radii have large error bars, all five of the inner planets have sub-Neptune radii, with KOI-351.07 being the outermost of these. The outer two planets appear to be gas giants. The new, seventh candidate was missed by the TPS algorithm, likely in part due to the unfortunate timing of data gaps in blocking four consecutive transits, although it was still detectable with three full transits and one partial in Q1-12. This may merit an increased scrutiny of known multiplanetary systems for additional high multiplicity systems.

Also noteworthy is the new planet candidate around KIC 2437209, which boasts a 71 hour transit every 281 days. While  $Y^2$  interpolation favors a large stellar radius, this long duration is also consistent with an extremely eccentric  $e = 0.98$  planet, a planet potentially undergoing high

eccentricity migration. However, follow-up analysis places KIC 2437209 on the giant branch of NGC 6791.

Several long period candidates are discovered too. However, many of these contain only two transits. With the failure of *Kepler*'s third reaction wheel, one and two transit systems become important in order to study cool planets orbiting far from their host stars. This is especially so for known planetary systems, since the probability that a false positive occurs in a known planetary system is much lower (Lissauer et al. 2012). Planet Hunters continue to collect one and two transit systems, and these will be further explored in a future paper, Picard et al. (2013, in preparation).

This paper brings the total new planetary candidates discovered by Planet Hunters to  $\sim 60$  plus the two confirmed planets, PH1 b and PH2 b, and new candidates continue to be passed to the science team. As the last *Kepler* data are released, Planet Hunters will continue their search for more planetary candidates.

#### *Acknowledgements*

We thank all Planet Hunter volunteers, who were indispensable for their work in discovering and analyzing planet candidates in this paper. All Planet Hunters are individually acknowledged at <http://www.planethunters.org/authors>.

DF acknowledges funding support for PlanetHunters.org from Yale University and support from the NASA Supplemental Outreach Award, 10-OUTRCH.210-0001 and the NASA ADAP12-0172. TSB acknowledges support provided through NASA grant ADAP12-0172. KS gratefully acknowledges support from Swiss National Science Foundation Grant PP00P2\_138979/1. Planet Hunters is partially supported by NASA JPL's PlanetQuest program. The Talk system was supported by the National Science Foundation under Grant No. DRL-0941610. The Zooniverse Project is supported by The Leverhulme Trust and by the Alfred P. Sloan foundation. We have used public data from NASA/IPAC/NEExSci Star and the Exoplanet Database, which is maintained by JPL at Caltech, under contract with NASA. Our research has utilized NASA's Astrophysics Data System Bibliographic Services. We acknowledge the *Kepler* science team and others involved for their great and ongoing work. Funding for the *Kepler* mission is provided by the NASA Science Mission directorate. The publicly released *Kepler* light curves were downloaded from the Multimission Archive at the Space Telescope Science Institute (MAST). STScI is operated by the Association of Universities for Research in Astronomy, Inc., under NASA contract NAS5-26555. Support for MAST for non-HST data is provided by the NASA Office of Space Science via grant NNX09AF08G and by other grants and contracts. This work made use of PyKE, a software package for the reduction and analysis of *Kepler* data. This open source software project is developed and distributed by the NASA *Kepler* Guest Observer Office.



## REFERENCES

- Agol, E., Steffen, J., Sari, R., & Clarkson, W. 2005, *MNRAS*, 359, 567
- Anglada-Escudé, G., et al. 2013, *A&A*, 556, A126
- Basu, S., Verner, G. A., Chaplin, W. J., & Elsworth, Y. 2012, *ApJ*, 746, 76
- Batalha, N. M., et al. 2010, *ApJ*, 713, L103
- . 2013, *ApJS*, 204, 24
- Borucki, W. J., et al. 2010, *Science*, 327, 977
- . 2011, *ApJ*, 736, 19
- . 2013, *Science*, 340, 587
- Brown, T. M., Latham, D. W., Everett, M. E., & Esquerdo, G. A. 2011, *AJ*, 142, 112
- Bryson, S. T., et al. 2013, *ArXiv e-prints*
- Carter, J. A., & Winn, J. N. 2009, *ApJ*, 704, 51
- Claret, A., & Bloemen, S. 2011, *A&A*, 529, A75
- Demarque, P., Woo, J.-H., Kim, Y.-C., & Yi, S. K. 2004, *ApJS*, 155, 667
- Eastman, J., Gaudi, B. S., & Agol, E. 2013, *PASP*, 125, 83
- Fischer, D. A., et al. 2008, *ApJ*, 675, 790
- . 2012, *MNRAS*, 419, 2900
- Fortson, L., et al. 2012, in *Advances in Machine Learning and Data Mining for Astronomy*, CRC Press, Taylor & Francis Group, Eds.: Michael J. Way, Jeffrey D. Scargle, Kamal M. Ali, Ashok N. Srivastava, p. 213-236, ed. M. J. Way, J. D. Scargle, K. M. Ali, & A. N. Srivastava, 213–236
- Fressin, F., et al. 2012, *Nature*, 482, 195
- . 2013, *ApJ*, 766, 81
- Gazak, Z., Johnson, J. A., Tonry, J., Eastman, J., Mann, A. W., & Agol, E. 2011, *ArXiv e-prints*
- Holman, M. J., & Murray, N. W. 2005, *Science*, 307, 1288
- Holman, M. J., et al. 2010, *Science*, 330, 51
- Jenkins, J. M., Caldwell, D. A., & Borucki, W. J. 2002, *ApJ*, 564, 495

- Jenkins, J. M., et al. 2010, in Society of Photo-Optical Instrumentation Engineers (SPIE) Conference Series, Vol. 7740, Society of Photo-Optical Instrumentation Engineers (SPIE) Conference Series
- Lintott, C., et al. 2011, MNRAS, 410, 166
- Lintott, C. J., et al. 2008, MNRAS, 389, 1179
- . 2013, AJ, 145, 151
- Lissauer, J. J., et al. 2011a, Nature, 470, 53
- . 2011b, ApJS, 197, 8
- . 2012, ApJ, 750, 112
- Lovis, C., et al. 2011, A&A, 528, A112
- Mazeh, T., et al. 2013, ApJS, 208, 16
- Miralda-Escudé, J. 2002, ApJ, 564, 1019
- Morton, T. D., & Johnson, J. A. 2011, ApJ, 738, 170
- Muirhead, P. S., Hamren, K., Schlawin, E., Rojas-Ayala, B., Covey, K. R., & Lloyd, J. P. 2012, ApJ, 750, L37
- Pinsonneault, M. H., An, D., Molenda-Żakowicz, J., Chaplin, W. J., Metcalfe, T. S., & Bruntt, H. 2012, ApJS, 199, 30
- Platais, I., Cudworth, K. M., Kozhurina-Platais, V., McLaughlin, D. E., Meibom, S., & Veillet, C. 2011, ApJ, 733, L1
- Schwamb, M. E., et al. 2012, ApJ, 754, 129
- . 2013, ApJ, 768, 127
- Seager, S. 2010, Exoplanet Atmospheres: Physical Processes
- Socrates, A., Katz, B., Dong, S., & Tremaine, S. 2012, ApJ, 750, 106
- Still, M., & Barclay, T. 2012, Astrophysics Source Code Library, 8004
- Swift, J. J., Johnson, J. A., Morton, T. D., Crepp, J. R., Montet, B. T., Fabrycky, D. C., & Muirhead, P. S. 2013, ApJ, 764, 105
- Tenenbaum, P., Bryson, S. T., Chandrasekaran, H., Li, J., Quintana, E., Twicken, J. D., & Jenkins, J. M. 2010, in Society of Photo-Optical Instrumentation Engineers (SPIE) Conference Series, Vol. 7740, Society of Photo-Optical Instrumentation Engineers (SPIE) Conference Series

Tenenbaum, P., et al. 2012, ArXiv e-prints

Tuomi, M. 2012, A&A, 543, A52

Valenti, J. A., & Fischer, D. A. 2005, ApJS, 159, 141

Valenti, J. A., & Piskunov, N. 1996, A&AS, 118, 595

Verner, G. A., et al. 2011, ApJ, 738, L28

Vogt, S. S., et al. 1994, in Society of Photo-Optical Instrumentation Engineers (SPIE) Conference Series, Vol. 2198, Society of Photo-Optical Instrumentation Engineers (SPIE) Conference Series, 362–+

Wang, J., et al. 2013, ApJ, 776, 10

Wright, J. T., et al. 2011, PASP, 123, 412

Table 1. Stellar Parameters

Star (KIC)	$K_p$ (mag)	Input Values			Derived Values					
		$(g-r)$ (mag)	$T_{\text{eff}}$ (K)	[Fe/H] (dex)	$T_{\text{eff}}$ (K)	$\log g$ (cgs)	$M_*$ ( $M_\odot$ )	$R_*$ ( $R_\odot$ )	$L_*$ ( $L_\odot$ )	$\rho_*$ ( $\text{g cm}^{-3}$ )
2437209 <sup>a</sup>	16.353	1.001	4655	-0.05	4675 <sup>+116</sup> <sub>-197</sub>	2.95 <sup>+0.13</sup> <sub>-0.10</sub>	1.10 <sup>+0.20</sup> <sub>-0.26</sub>	5.30 <sup>+0.98</sup> <sub>-0.97</sub>	8.19 <sup>+4.28</sup> <sub>-1.89</sub>	0.01 ± 0.01
5010054 <sup>a</sup>	13.961	0.631	5492	0.00	5550 <sup>+201</sup> <sub>-204</sub>	3.72 <sup>+0.11</sup> <sub>-0.10</sub>	1.05 <sup>+0.15</sup> <sub>-0.21</sub>	2.17 <sup>+0.40</sup> <sub>-0.45</sub>	2.28 <sup>+1.25</sup> <sub>-1.13</sub>	0.14 ± 0.09
5094412 <sup>a</sup>	15.772	0.633	5319	-0.33	5313 <sup>+154</sup> <sub>-253</sub>	4.53 <sup>+0.10</sup> <sub>-0.17</sub>	0.82 <sup>+0.09</sup> <sub>-0.10</sub>	0.80 <sup>+0.12</sup> <sub>-0.12</sub>	0.33 <sup>+0.15</sup> <sub>-0.19</sub>	2.26 ± 1.05
5522786 <sup>a</sup>	9.350	-0.146	8717	-0.03	8719 <sup>+194</sup> <sub>-190</sub>	4.30 <sup>+0.22</sup> <sub>-0.30</sub>	1.79 <sup>+0.34</sup> <sub>-0.31</sub>	1.30 <sup>+0.57</sup> <sub>-0.29</sub>	8.82 <sup>+9.38</sup> <sub>-4.09</sub>	1.16 ± 1.17
5732155 <sup>a</sup>	15.195	0.550	5879	-0.03	5755 <sup>+155</sup> <sub>-429</sub>	3.85 <sup>+0.16</sup> <sub>-0.13</sub>	1.13 <sup>+0.14</sup> <sub>-0.22</sub>	1.99 <sup>+0.36</sup> <sub>-0.44</sub>	2.26 <sup>+1.32</sup> <sub>-0.49</sub>	0.20 ± 0.13
6372194 <sup>a</sup>	15.870	0.698	5138	-0.37	5233 <sup>+180</sup> <sub>-174</sub>	4.57 <sup>+0.10</sup> <sub>-0.11</sub>	0.80 <sup>+0.09</sup> <sub>-0.09</sub>	0.75 <sup>+0.11</sup> <sub>-0.11</sub>	0.30 <sup>+0.10</sup> <sub>-0.19</sub>	2.70 ± 1.25
6436029 <sup>a</sup>	15.768	1.007	4652	0.41	4697 <sup>+194</sup> <sub>-220</sub>	4.62 <sup>+0.10</sup> <sub>-0.10</sub>	0.79 <sup>+0.09</sup> <sub>-0.08</sub>	0.72 <sup>+0.10</sup> <sub>-0.09</sub>	0.16 <sup>+0.08</sup> <sub>-0.10</sub>	2.94 ± 1.16
6805414 <sup>a</sup>	15.392	0.555	5802	-0.08	5677 <sup>+140</sup> <sub>-330</sub>	3.69 <sup>+0.11</sup> <sub>-0.10</sub>	1.06 <sup>+0.13</sup> <sub>-0.20</sub>	1.64 <sup>+0.34</sup> <sub>-0.16</sub>	3.23 <sup>+1.45</sup> <sub>-1.43</sub>	0.34 ± 0.16
9662267 <sup>a</sup>	14.872	0.534	5765	-0.03	5602 <sup>+151</sup> <sub>-531</sub>	4.42 <sup>+0.11</sup> <sub>-0.42</sub>	0.86 <sup>+0.13</sup> <sub>-0.18</sub>	0.89 <sup>+0.19</sup> <sub>-0.27</sub>	0.66 <sup>+0.35</sup> <sub>-0.36</sub>	1.69 ± 1.33
9704149 <sup>a</sup>	15.102	0.540	5639	-0.16	5640 <sup>+181</sup> <sub>-181</sub>	4.47 <sup>+0.10</sup> <sub>-0.38</sub>	0.86 <sup>+0.11</sup> <sub>-0.14</sub>	0.78 <sup>+0.15</sup> <sub>-0.22</sub>	0.47 <sup>+0.25</sup> <sub>-0.25</sub>	2.53 ± 1.80
10255705 <sup>a</sup>	12.950	0.698	5094	-0.13	5039 <sup>+143</sup> <sub>-389</sub>	3.74 <sup>+0.16</sup> <sub>-0.21</sub>	1.10 <sup>+0.17</sup> <sub>-0.29</sub>	2.12 <sup>+0.52</sup> <sub>-0.44</sub>	2.44 <sup>+1.37</sup> <sub>-0.78</sub>	0.16 ± 0.11
11152511 <sup>a</sup>	13.618	0.640	5314	-0.10	5273 <sup>+145</sup> <sub>-471</sub>	3.81 <sup>+0.10</sup> <sub>-0.10</sub>	1.01 <sup>+0.15</sup> <sub>-0.18</sub>	2.08 <sup>+0.30</sup> <sub>-0.45</sub>	2.83 <sup>+0.91</sup> <sub>-1.23</sub>	0.16 ± 0.09
11442793 <sup>b</sup>	13.804	0.398	6317	-0.11	6157 <sup>+162</sup> <sub>-417</sub>	4.34 <sup>+0.10</sup> <sub>-0.12</sub>	1.13 <sup>+0.06</sup> <sub>-0.18</sub>	1.14 <sup>+0.07</sup> <sub>-0.13</sub>	1.60 <sup>+0.49</sup> <sub>-0.56</sub>	1.07 ± 0.31
12454613 <sup>a</sup>	13.537	0.617	5335	0.03	5420 <sup>+331</sup> <sub>-158</sub>	4.52 <sup>+0.10</sup> <sub>-0.12</sub>	0.87 <sup>+0.09</sup> <sub>-0.14</sub>	0.82 <sup>+0.12</sup> <sub>-0.20</sub>	0.39 <sup>+0.18</sup> <sub>-0.23</sub>	2.23 ± 1.31

<sup>a</sup>Brown et al. (2011).<sup>b</sup>Pinsonneault et al. (2012).

Note. — Stellar inputs (left hand side) and outputs (right hand side) from iterative light curve and stellar isochrone fitting routine. See Section 3.2 for details.

Table 2. Orbital Parameters

Star (KIC)	$T_0$ (MJD)	Period (d)	Impact Parameter	$R_{PL}/R_*$	e	$\omega$ (radian)	$i$ (deg)	$a/R_*$	a (AU)	$R_{PL}$ ( $R_{\oplus}$ )	$T_{PL}$ (K)	Depth (ppm)	Duration (hours)
2437209*	55047.9340	281.2228 <sup>+0.0001</sup> <sub>-0.0017</sub>	0.40 <sup>+0.13</sup> <sub>-0.36</sub>	0.1070 <sup>+0.0027</sup> <sub>-0.0020</sub>	0.00 <sup>+0.00</sup> <sub>-0.00</sub>	0.00 <sup>+0.00</sup> <sub>-0.00</sub>	89.27 <sup>+0.39</sup> <sub>-0.28</sub>	31.02 <sup>+2.44</sup> <sub>-2.66</sub>	0.87 ± 0.06	61.86 ± 11.46	557 ± 30	14005 ± 1036	71.24
5010054 <sup>†</sup>	55188.8990	904.2400 <sup>+0.0113</sup> <sub>-0.0146</sub>	0.79 <sup>+0.21</sup> <sub>-0.79</sub>	0.0293 <sup>+0.0041</sup> <sub>-0.0028</sub>	0.00 <sup>+0.00</sup> <sub>-0.00</sub>	0.00 <sup>+0.46</sup> <sub>-0.00</sub>	89.79 <sup>+0.20</sup> <sub>-0.05</sub>	216.39 <sup>+187.47</sup> <sub>-34.37</sub>	1.86 ± 0.11	6.94 ± 1.59	251 ± 65	825 ± 135	20.65
5094412*	55009.0210	276.8800 <sup>+0.0319</sup> <sub>-0.0258</sub>	0.98 <sup>+0.02</sup> <sub>-0.20</sub>	0.0650 <sup>+0.0532</sup> <sub>-0.0395</sub>	0.00 <sup>+0.05</sup> <sub>-0.00</sub>	0.00 <sup>+0.08</sup> <sub>-0.00</sub>	89.74 <sup>+0.21</sup> <sub>-0.73</sub>	218.09 <sup>+14.73</sup> <sub>-30.62</sub>	0.78 ± 0.03	5.68 ± 4.14	239 ± 15	2009 ± 281	3.92
5522786 <sup>†</sup>	55115.4980	757.1639 <sup>+0.1629</sup> <sub>-0.0588</sub>	0.63 <sup>+0.15</sup> <sub>-0.63</sub>	0.0090 <sup>+0.0003</sup> <sub>-0.0004</sub>	0.56 <sup>+0.14</sup> <sub>-0.27</sub>	0.35 <sup>+1.37</sup> <sub>-0.35</sub>	89.86 <sup>+0.14</sup> <sub>-0.04</sub>	255.68 <sup>+7.21</sup> <sub>-18.76</sub>	1.98 ± 0.12	1.27 ± 0.42	362 ± 12	91 ± 13	14.43
5732155 <sup>†</sup>	55369.2000	644.1695 <sup>+0.0014</sup> <sub>-0.0014</sub>	0.67 <sup>+0.14</sup> <sub>-0.18</sub>	0.0585 <sup>+0.0037</sup> <sub>-0.0011</sub>	0.00 <sup>+0.05</sup> <sub>-0.00</sub>	0.00 <sup>+0.06</sup> <sub>-0.00</sub>	89.76 <sup>+0.08</sup> <sub>-0.10</sub>	161.32 <sup>+26.64</sup> <sub>-18.46</sub>	1.52 ± 0.08	12.70 ± 2.62	301 ± 26	3648 ± 404	24.53
6372194*	55375.9140	281.5848 <sup>+0.0037</sup> <sub>-0.0031</sub>	0.89 <sup>+0.11</sup> <sub>-0.28</sub>	0.1011 <sup>+0.0013</sup> <sub>-0.0075</sub>	0.65 <sup>+0.05</sup> <sub>-0.24</sub>	0.00 <sup>+0.60</sup> <sub>-0.00</sub>	89.69 <sup>+0.05</sup> <sub>-0.11</sub>	232.18 <sup>+8.50</sup> <sub>-8.64</sub>	0.78 ± 0.03	8.26 ± 1.28	228 ± 9	10507 ± 355	5.72
6436029	55290.6000	505.4500 <sup>+0.0042</sup> <sub>-0.0043</sub>	0.34 <sup>+0.66</sup> <sub>-0.34</sub>	0.0387 <sup>+0.0108</sup> <sub>-0.0013</sub>	0.00 <sup>+0.07</sup> <sub>-0.00</sub>	0.00 <sup>+0.10</sup> <sub>-0.00</sub>	89.94 <sup>+0.06</sup> <sub>-0.39</sub>	315.86 <sup>+29.32</sup> <sub>-187.56</sub>	1.15 ± 0.04	3.06 ± 0.61	175 ± 31	1883 ± 391	11.77
6805414*	55137.9500	200.2490 <sup>+0.0010</sup> <sub>-0.0011</sub>	0.48 <sup>+0.13</sup> <sub>-0.16</sub>	0.1043 <sup>+0.0026</sup> <sub>-0.0018</sub>	0.00 <sup>+0.00</sup> <sub>-0.00</sub>	0.00 <sup>+0.00</sup> <sub>-0.00</sub>	89.58 <sup>+0.13</sup> <sub>-0.17</sub>	65.93 <sup>+4.71</sup> <sub>-6.45</sub>	0.68 ± 0.04	18.71 ± 2.82	464 ± 27	12456 ± 306	22.82
9662267 <sup>†</sup>	55314.3800	466.2020 <sup>+0.0118</sup> <sub>-0.0115</sub>	0.79 <sup>+0.14</sup> <sub>-0.08</sub>	0.0390 <sup>+0.0076</sup> <sub>-0.0019</sub>	0.11 <sup>+0.41</sup> <sub>-0.11</sub>	0.03 <sup>+0.58</sup> <sub>-0.03</sub>	89.82 <sup>+0.03</sup> <sub>-0.06</sub>	248.53 <sup>+17.42</sup> <sub>-25.00</sub>	1.12 ± 0.07	3.80 ± 1.07	236 ± 18	1501 ± 225	9.41
9704149 <sup>†</sup>	55252.2220	697.0159 <sup>+0.0058</sup> <sub>-0.0055</sub>	0.33 <sup>+0.36</sup> <sub>-0.33</sub>	0.0519 <sup>+0.0015</sup> <sub>-0.0006</sub>	0.29 <sup>+0.17</sup> <sub>-0.28</sub>	0.13 <sup>+0.56</sup> <sub>-0.13</sub>	89.95 <sup>+0.05</sup> <sub>-0.03</sub>	348.03 <sup>+17.43</sup> <sub>-30.09</sub>	1.46 ± 0.07	4.43 ± 1.03	201 ± 9	3235 ± 407	13.86
10255705 <sup>†</sup>	55378.2500	707.3793 <sup>+0.0157</sup> <sub>-0.0039</sub>	0.56 <sup>+0.25</sup> <sub>-0.35</sub>	0.0315 <sup>+0.0149</sup> <sub>-0.0027</sub>	0.00 <sup>+0.10</sup> <sub>-0.00</sub>	0.00 <sup>+0.00</sup> <sub>-0.00</sub>	89.75 <sup>+0.15</sup> <sub>-0.17</sub>	128.50 <sup>+22.92</sup> <sub>-23.81</sub>	1.60 ± 0.11	7.31 ± 2.57	295 ± 31	1029 ± 127	36.29
11152511	55193.2608	287.3630 <sup>+0.0136</sup> <sub>-0.0433</sub>	0.86 <sup>+0.09</sup> <sub>-0.46</sub>	0.0175 <sup>+0.0085</sup> <sub>-0.0152</sub>	0.67 <sup>+0.02</sup> <sub>-0.63</sub>	0.65 <sup>+3.73</sup> <sub>-0.46</sub>	89.39 <sup>+0.61</sup> <sub>-0.59</sub>	80.53 <sup>+113.13</sup> <sub>-7.37</sub>	0.85 ± 0.05	3.97 ± 2.79	390 ± 148	372 ± 94	13.49
11442793*	55087.2210	124.9198 <sup>+0.0113</sup> <sub>-0.0166</sub>	0.88 <sup>+0.07</sup> <sub>-0.26</sub>	0.0224 <sup>+0.0139</sup> <sub>-0.0033</sub>	0.01 <sup>+0.02</sup> <sub>-0.01</sub>	0.00 <sup>+0.07</sup> <sub>-0.00</sub>	88.90 <sup>+0.81</sup> <sub>-0.74</sub>	45.96 <sup>+35.57</sup> <sub>-5.58</sub>	0.51 ± 0.02	2.80 ± 1.10	592 ± 136	446 ± 93	10.59
12454613 <sup>†</sup>	55322.7620	736.5100 <sup>+0.0065</sup> <sub>-0.0064</sub>	0.52 <sup>+0.47</sup> <sub>-0.14</sub>	0.0295 <sup>+0.0087</sup> <sub>-0.0008</sub>	0.00 <sup>+0.21</sup> <sub>-0.00</sub>	0.00 <sup>+0.03</sup> <sub>-0.00</sub>	89.92 <sup>+0.03</sup> <sub>-0.40</sub>	368.65 <sup>+19.59</sup> <sub>-54.09</sub>	1.52 ± 0.06	2.64 ± 0.66	187 ± 13	1006 ± 143	13.24

Note. — Planet candidates with only two transits are marked with a <sup>†</sup>. Of these, KIC 9704149 actually only has 1.5 transits due to a data gap interrupting the second transit. PH detections completely missed by TPS are marked with a \*.

Table 3. Nearest linear ephemerides of KOI-351’s previously known candidates to KOI-351.07

	<b>T0</b> 254.64	<b>Phase</b> Difference	<b>T2</b> 504.57 <sup>†</sup>	<b>Phase</b> Difference	<b>T5</b> 879.27	<b>Phase</b> Difference	<b>T6</b> 1004.17	<b>Phase</b> Difference	<b>T8</b> 1253.97	<b>Phase</b> Difference	<b>T9</b> 1378.87	<b>Phase</b> Difference	<b>Depth</b> (ppm)	<b>Duration</b> (hours)
KOI-351.01	140.48	...	472.12	...	803.76	...	803.76	...	1135.41	...	1135.41	...	8423	14.53
KOI-357.07	254.64	0.34	504.57	0.10	879.27	0.23	1004.17	0.60	1253.97	0.36	1378.87	0.73	433	10.75
KOI-351.01	472.12	...	803.76	...	1135.41	...	1135.41	...	1467.41	...	1467.41	...	...	...
KOI-351.02	147.05	...	357.66	...	778.87	...	989.47	...	1200.08	...	1200.08	...	4150	11.69
KOI-357.07	254.64	0.51	504.57	0.70	879.27	0.48	1004.17	0.07	1253.97	0.26	1378.87	0.85	433	10.75
KOI-351.02	357.66	...	568.26	...	989.47	...	1200.08	...	1410.68	...	1410.68	...	...	...
KOI-351.03	218.69	...	457.65	...	875.83	...	995.31	...	1234.27	...	1353.75	...	587	8.07
KOI-357.07	254.64	0.60	504.57	0.79	879.27	0.06	1004.17	0.15	1253.97	0.33	1378.87	0.42	433	10.75
KOI-351.03	278.43	...	517.39	...	935.57	...	1055.05	...	1294.01	...	1413.49	...	...	...
KOI-351.04	226.25	...	502.06	...	869.80	...	961.74	...	1237.55	...	1329.48	...	410	6.42
KOI-357.07	254.64	0.31	504.57	0.03	879.27	0.10	1004.17	0.46	1253.97	0.18	1378.87	0.54	433	10.75
KOI-351.04	318.19	...	594.00	...	961.74	...	1053.68	...	1329.48	...	1421.42	...	...	...
KOI-351.05	252.84	...	497.00	...	871.96	...	1002.76	...	1246.92	...	1377.72	...	116	3.69
KOI-357.07	254.64	0.21	504.57	0.87	879.27	0.84	1004.17	0.16	1253.97	0.81	1378.87	0.13	433	10.75
KOI-351.05	261.56	...	505.72	...	880.68	...	1011.48	...	1255.64	...	1386.44	...	...	...
KOI-351.06	249.80	...	502.10	...	873.54	...	999.69	...	1251.99	...	1378.14	...	91	3.80
KOI-357.07	254.64	0.69	504.57	0.35	879.27	0.82	1004.17	0.64	1253.97	0.28	1378.87	0.10	433	10.75
KOI-351.06	256.81	...	509.11	...	880.55	...	1006.70	...	1259.00	...	1385.15	...	...	...

Note. — <sup>†</sup> Transit 5 (T5) is only a partial transit. A data gap within quarter 5 blocks out everything but the egress. Missing transits T1, T3, T4, and T7, fell into data gaps. Midtransit times of our new KOI-351.07 sandwiched between the nearest two midtransit times of all other six candidates in the system, according to a linear ephemeris as calculated by the NASA Exoplanet Archive’s Exoplanet Transit Ephemeris Service (<http://exoplanetarchive.ipac.caltech.edu/applications/TransitSearch/>). The only midtransit of KOI-351.07 falling within one day of any other transit in the system occurs for KOI-351.06 for Transit 9 (T9), the planet with the shortest period, and thus the one most likely to fall within a day of KOI-351.07 by chance, although its midtransit still falls 17 hours too early. All times are measured in Barycentric Julian Day (BJD) - 2454833.00 days. We also show the phase of midtransit of KOI-351.07 relative to the period of the other six candidates and demonstrate that this is not a secondary eclipse of another object.

Table 4. KOI-351 Candidates

Candidate	$T_0$ (MJD)	Period (d)	Impact Parameter	$R_{\text{PL}}/R_*$	$i$ (deg)	$a/R_*$	$a$ (AU)	$R_{\text{PL}}$ ( $R_{\oplus}$ )	$T_{\text{PL}}$ (K)	Depth (ppm)	Duration (hours)
KOI-351.01	54972.9774	331.64	0.331	0.084	89.95	179.93	0.98	$9.8 \pm 4.3$	292	8423	14.53
KOI-351.02	54979.5513	210.61	0.435	0.0597	89.95	132.93	0.724	$7 \pm 3.1$	340	4150	11.69
KOI-351.03	54991.4538	59.74	0.115	0.0219	89.95	57.39	0.312	$2.6 \pm 1.3$	518	587	8.07
KOI-351.04	54966.8151	91.94	0.743	0.0202	89.38	76.50	0.416	$2.4 \pm 1.4$	448	410	6.42
KOI-351.05	54971.9758	8.72	0.494	0.0101	88.24	15.91	0.087	$1.18 \pm 0.51$	981	116	3.69
KOI-351.06	54970.1658	7.01	0.26	0.0087	88.81	13.75	0.075	$1.02 \pm 0.44$	1056	91	3.80
KOI-351.07	55087.2210	124.92	0.88	0.0224	88.90	45.66	0.51	$2.80 \pm 1.10$	592	446	10.59

Note. — KOI-351.01 through KOI-351.06 values are directly from the the public KOI data (<http://exoplanetarchive.ipac.caltech.edu>, last accessed September 23, 2013), which has stellar parameters  $M = 1.14 \pm 0.12 M_{\odot}$ ,  $R = 1.07 \pm 0.46 R_{\odot}$ , and  $T_{\text{eff}} = 6330 K$ . KOI-351.07 values are from our fit using our model’s stellar parameters of  $M = 1.13^{+0.09}_{-0.18} M_{\odot}$ ,  $R = 1.14^{+0.07}_{-0.13} R_{\odot}$ , and  $T_{\text{eff}} = 6042 K$ .